Korean J. Chem. Eng., **26**(4), 930-934 (2009)
DOI: 10.1007/s11814-009-0156-0

Stability of buoyancy-driven convection in directional solidification of a binary melt

In Gook Hwang*,† and Chang Kyun Choi**

*Department of Chemical and Biochemical Engineering, The University of Suwon, Gyeonggi-do 445-743, Korea
**School of Chemical and Biological Engineering, Seoul National University, Seoul 151-744, Korea
(*Received 30 April 2008 • accepted 20 January 2009*)

Abstract−In directional solidification, compositional convection can be driven by an unstable density gradient in the melt. In this paper convective instabilities in liquid and mushy layers during solidification of a horizontal binary melt are analyzed by using the propagation theory. The self-similar stability equations are used to examine the boundary-mode and mushy-layer-mode of convection. The effects of velocity conditions at the liquid-mush interface on the onset of convection are discussed. The critical Darcy-Rayleigh number for the convection in the mushy layer decreases with increasing the temperature of a cooled boundary.

Key words: Directional Solidification, Buoyancy-driven Convection, Propagation Theory, Self-similar Stability Analysis

INTRODUCTION

In a binary solidification, a two-component melt is solidified from a cooled boundary and its compositional profile develops with time by solute injection or incorporation at a solid-liquid interface. Natural convection can occur both in an unstable compositional boundary layer and in a mushy layer, resulting in freckles in solidified alloys [1-4]. The dendritic mush is a region of solid-liquid mixed phase formed between the melt and solid layers. The Darcy-Rayleigh number for the onset of convection in a mushy layer, defined by $R_m^*=g\beta_m\Delta C\Pi H/(\kappa\nu)$, is an important parameter in the study of the channel formation [5-9].

In steady solidification models, in which the melt solidifies upwards with a constant velocity, Worster [6] analyzed two modes of convection in binary alloys: the boundary-layer-mode and mushy-layer-mode of instabilities. The convection in a mushy layer has been studied theoretically using the steady solidification model [10-13]. The stability of plume convection, which is an up-flow in the mush, is studied by using the equations in the mush decoupled from the liquid layer [8,14]. In time-dependent solidification models, in which the mushy layer grows from a bottom boundary, Emms and Fowler [9] studied the onset of convection in the mush using the simplified model based on the quasi-static stability analysis. Chen and Chen [5] experimentally determined the onset conditions of plume convection for various bottom temperatures and estimated the critical solute Rayleigh number across the mushy layer. The onset of compositional convection during time-dependent solidification was analyzed by the propagation theory [15-17].

The propagation theory [18-25] determines the critical conditions for the onset of convection by using the thermal penetration depth as a length scaling factor. Recently, Choi et al. [25] investigated the temporal evolution of disturbances in a fluid layer heated from below and predicted the onset of thermal instability, based on the growth rates of the basic temperature field and its fluctuations. In this paper, we study the critical conditions for the convection in the liquid and mushy layers during binary solidification, applying the Beavers-Joseph condition to the liquid adjacent to the liquid-mush interface [26]. The time-dependent disturbance equations for the liquid and mushy layers are transformed to the self-similar stability equations by using a similarity variable [17]. The critical Darcy-Rayleigh numbers for the convection in the mushy layer are predicted as a function of the temperature of the bottom boundary in solidification of aqueous ammonium chloride (NH_4Cl-H_2O) solution.

PROPAGATION THEORY

The governing equations for convection during solidification of a binary melt are well established in previous studies [6,9]. Consider the directional solidification system in which a mushy layer is growing from below, as shown in Fig. 1. The supereutectic melt is

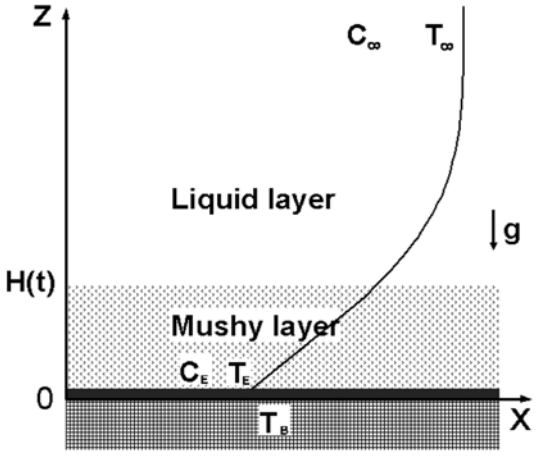

Fig. 1. Schematic diagram of liquid and mushy layers in directional solidification system.

†To whom correspondence should be addressed.
E-mail: ighwang@suwon.ac.kr
‡This paper is presented on the occasion of professor Chang Kyun Choi's retirement from the school of chemical and biological engineering of Seoul National University.

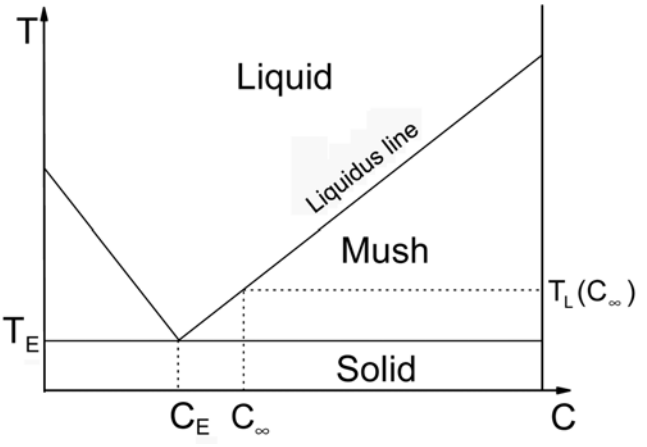

Fig. 2. Schematic phase diagram of binary melt.

initially quiescent at a constant temperature, T_∞, and a constant solute concentration, C_∞. For time $t\geq 0$ the bottom boundary of the melt is cooled at a constant temperature T_B. The mushy layer grows above a eutectic solid layer, and compositional convection of light residual liquid may be induced. When the temperature of the bottom boundary is lower than the eutectic temperature, T_E, the bottom boundary of the mush is assumed to be at the eutectic temperature, T_E, and the eutectic composition, C_E. The position of the mush-liquid interface $H(=2\lambda\sqrt{\kappa t})$ is moving upward, where λ is the phase-change rate of the mushy layer and κ is the thermal diffusivity. In the mushy layer the liquidus temperature T_L is given by

$$T_L-T_L(C_\infty)=\Gamma(C-C_\infty), \tag{1}$$

where Γ is the slope of the liquidus curve. The schematic phase diagram of a binary melt is shown in Fig. 2, which is similar to the system of aqueous ammonium chloride solution.

The non-dimensional disturbance equations for the liquid layer, derived from linear stability theory, are given in Hwang and Choi [17]:

$$\frac{\partial\theta_1}{\partial\tau}+R_T w_1\frac{\partial\theta_0}{\partial z}=\nabla^2\theta_1, \tag{2}$$

$$\frac{\partial c_1}{\partial\tau}+R_S w_1\frac{\partial c_0}{\partial z}=Le\nabla^2 c_1, \tag{3}$$

$$\left(\frac{1}{Pr}\frac{\partial}{\partial\tau}-\nabla^2\right)\nabla^2 w_1=\left(\frac{\partial^2}{\partial x^2}+\frac{\partial^2}{\partial y^2}\right)(\theta_1-c_1). \tag{4}$$

The non-dimensional disturbance equations for the mushy layer are

$$\frac{\partial\theta_{m1}}{\partial\tau}+R_m w_{m1}\frac{\partial\theta_{m0}}{\partial z}=\nabla^2\theta_{m1}-St\frac{\partial\chi}{\partial\tau}, \tag{5}$$

$$\chi_1\frac{\partial\theta_{m0}}{\partial\tau}+\chi_0\frac{\partial\theta_{m1}}{\partial\tau}+R_m w_1\frac{\partial\theta_{m0}}{\partial z}=(\gamma-\theta_{m0})\frac{\partial\chi_1}{\partial\tau}-\theta_{m1}\frac{\partial\chi_0}{\partial\tau}, \tag{6}$$

$$\nabla^2 w_{m1}=-\left(\frac{\partial^2}{\partial x^2}+\frac{\partial^2}{\partial y^2}\right)\theta_{m1}, \tag{7}$$

where w is the vertical velocity component, x and y are the horizontal coordinates, and τ is the time. The distances have been scaled with an arbitrary length L, the time with L^2/κ, and the velocity with κ/L. The depth of a binary melt is usually chosen as the length scale L. However, in the present system the liquid layer is assumed to be semi-infinite and the length scale L is defined as an arbitrary one. The temperature and concentration are defined by $\theta=(T-T_L(C_\infty))/\Delta T$ and $c=(C-C_\infty)/\Delta C$, respectively, where $\Delta T=\Gamma\Delta C=T_L(C_\infty)-T_E$ and $\Delta C=C_\infty-C_E$. In the liquid layer, the perturbed temperature θ_1 has the scale of $\kappa\nu/(g\alpha L^3)$, and c_1 has the scale of $\kappa\nu/(g\beta L^3)$. In the mushy layer, the perturbed quantities θ_{m1}, w_{m1}, and χ_1 have the scale of $\kappa\nu\Gamma/(g\beta_m L^3)$, $\Pi\kappa/L^3$, and $\kappa\nu/(g\beta_m\Delta C L^3)$, respectively. The porosity profile in the mushy layer is given by $\chi_0=(\gamma-\theta_l)/(\gamma-\theta_{m0})$. The dimensionless parameter, Le, is the Lewis number (=D/κ), and Pr is the Prandtl number (=ν/κ), where D is the solute diffusivity, and ν is the kinematic viscosity. The thermal Rayleigh number is defined by $R_T=(g\alpha\Delta T L^3)/\kappa\nu$, and the solutal Rayleigh number is defined by $R_S=g\beta\Delta C L^3/\kappa\nu$, where g denotes the gravity acceleration, α and β and are the thermal and solutal expansion coefficients, respectively. The Darcy-Rayleigh number is defined by $R_m=g\beta_m\Delta C\Pi L/(\kappa\nu)$, where Π denotes the permeability of the mushy layer, assumed to be constant, and $\beta_m=\beta-\alpha\Gamma$. The parameter St is the Stefan number (=$\overline{L}/(C_P\Delta T)$) and γ is the concentration ratio (=$(C_s-C_\infty)/\Delta C$), where $\overline{L}$ denotes the latent heat of fusion, C_P the specific heat, and C_s the solute concentration in solid.

In propagation theory, the thermal or compositional penetration depth is used as a length scaling factor, and self-similarity is applied to the time-dependent disturbance equations. In this study the penetration depth ($\propto\tau^{1/2}$) and the mushy-layer thickness $h=2\lambda\tau^{1/2}$ are proportional to $\tau^{1/2}$, where λ is constant. For the self-similar transform the velocity disturbance w_1 in the liquid layer is rescaled with a time-dependent factor $h^2(\propto\tau)$, based on a scaling analysis [15]. The time-dependent disturbance equations are transformed to functions of a similarity variable $\zeta(=z/h=z/(2\lambda\tau^{1/2}))$ by using the mushy-layer thickness as a length scaling factor. The self-similar stability equations in the liquid layer are given by [17]

$$(\overline{D}^2+2\lambda^2\zeta\overline{D}-a^{*2})\theta^*=\frac{AR_m^*}{\Pi^*}w^*\overline{D}\theta_0, \tag{8}$$

$$(Le\overline{D}^2+2\lambda^2\zeta\overline{D}-Lea^{*2})c^*=\frac{(A+1)R_m^*}{\Pi^*}w^*\overline{D}c_0, \tag{9}$$

$$\left[(\overline{D}^2-a^{*2})^2+\frac{2\lambda^2}{Pr}(\zeta\overline{D}^3-a^{*2}\zeta\overline{D}+2a^{*2})\right]w^*=a^{*2}(\theta^*-c^*). \tag{10}$$

In the mushy layer the self-similar stability equations are given by

$$(\overline{D}^2+2\lambda^2\zeta\overline{D}-a^{*2})\theta_m^*=R_m^* w_m^*\overline{D}\theta_{m0}-2\lambda^2 St\zeta\overline{D}\chi^*, \tag{11}$$

$$2\lambda^2\zeta[\chi^*\overline{D}\theta_{m0}+\chi_0\overline{D}\theta_m^*+(\theta_{m0}-\gamma)\overline{D}\chi^*+\theta_m^*\overline{D}\chi_0]=R_m^* w_m^*\overline{D}\theta_{m0}, \tag{12}$$

$$(\overline{D}^2-a^{*2})w_m^*=a^{*2}\theta_m^*, \tag{13}$$

where $\overline{D}$ represents $d/d\zeta$ and a^* is the horizontal wave number. The vertical velocity disturbances w^* and w_m^* have the scale of $\kappa H^2/L^3$ and $\kappa\Pi/L^3$, respectively. The Darcy-Rayleigh number $R_m^*(=R_m h)$ based on the mushy layer thickness H is defined by

$$R_m^*=\frac{g\beta_m\Delta C\Pi H}{\kappa\nu}. \tag{14}$$

The Darcy number Π^* is defined by Π/H^2 and $A(=\Gamma\alpha/\beta_m)$ is the buoyancy ratio.

In the liquid layer, the basic-state temperature and concentration

fields are given by $\theta_0=\theta_\infty+(\theta_i-\theta_\infty)\mathrm{erfc}(\lambda\zeta)/\mathrm{erfc}(\lambda)$ and $c_0=\theta_i\mathrm{erfc}(\lambda\zeta\sqrt{\mathrm{Le}}/\mathrm{erfc}(\lambda/\sqrt{\mathrm{Le}})$, respectively, where $\theta_i(=(T_i-T_L(C_\infty))/\Delta T)$ is the temperature at the liquid-mush interface, and $\theta_\infty(=(T_\infty-T_L(C_\infty))/\Delta T)$ is the superheat. In the mushy layer, the basic-state equation and the boundary conditions are given by

$$\overline{D}^2\theta_{m0}+2\lambda^2\zeta\left(1+\mathrm{St}\frac{\gamma-\theta_i}{(\gamma-\theta_{m0})^2}\right)\overline{D}\theta_{m0}=0, \tag{15}$$

$$\theta_0=\theta_{m0},\ \overline{D}\theta_0=\overline{D}\theta_{m0}\ \text{at}\ \zeta=1, \tag{16a,b}$$

$$\theta_{m0}=-1\ \text{at}\ \zeta=0. \tag{17}$$

The following boundary conditions are applied to the self-similar stability equations:

for $\zeta\to\infty$

$$\theta^*=0,\ c^*=0,\ w^*=0,\ \overline{D}w^*=0, \tag{18a-d}$$

at $\zeta=1$

$$\theta^*=\frac{A}{1+A}c^*,\ \theta^*=A\theta_m^*, \tag{19a,b}$$

$$\overline{D}\theta^*=A\left[\frac{\overline{D}c^*}{1+A}-2\lambda^2\left(\frac{1-\mathrm{Le}}{\mathrm{Le}}\right)\overline{D}\theta_0 h^*\frac{R_m^*}{\Pi^*}\right], \tag{20}$$

$$\overline{D}\theta^*=A\left[\overline{D}\theta_m^*-2\lambda^2\left(\frac{\mathrm{St}}{\gamma}\right)\overline{D}\theta_0 h^*\frac{R_m^*}{\Pi^*}\right], \tag{21}$$

$$w^*=w_m^*\Pi^*,\ \chi^*=\frac{\overline{D}\theta_{m0}^*}{\theta_i-\gamma}h^*\frac{R_m^*}{\Pi^*}, \tag{22a,b}$$

$$\overline{D}^2w^*=B\left[\left(\frac{1}{\Pi^*}\right)^{1/2}(\overline{D}w^*-\Pi^*\overline{D}w_m^*)\right]\ \text{or}\ \overline{D}w^*=0, \tag{23 or 24}$$

$$\overline{D}w_m^*=-\left[\overline{D}^3w^*-a^{*2}\overline{D}w^*-\frac{2\lambda^2}{\mathrm{Pr}}(\overline{D}w^*-\overline{D}^2w^*)\right], \tag{25}$$

at $\zeta=0$

$$\theta_m^*=0,\ w_m^*=0, \tag{26a,b}$$

where $h^*(=-\Pi^*\theta_m^*/(R_m^*\overline{D}\theta_{m0})$ represents the perturbation to the position of the liquid-mush interface. Eq. (23) represents the Beavers-Joseph condition [26], and the constant B depends on experimental parameters, ranging from 0.1 to 4, and when the average pore size is large, the value of B is small [27]. In Hwang and Choi's [17] work the no-slip condition (24) is applied to the liquid adjacent to the liquid-mush interface. The Beavers-Joseph condition, which includes slip velocity at the liquid-mush interface, is a less restrictive condition than the no-slip condition. The shooting method is employed to solve the self-similar stability equations. The integration is performed from the liquid-mush interface to the bottom boundary and the fictitious distance satisfying the infinite boundary conditions.

RESULTS AND DISCUSSION

In this work, the stability criteria for $\Pi^*=10^{-5}$ and Pr=10 are investigated. The stabilizing thermal buoyancy is not considered by assuming A→0. The marginal stability curves for St=5, γ=20, θ_∞=0.8 and Le=0.013 are shown in Fig. 3 when the Beavers-Joseph condition (23) is applied to the liquid-mush interface. These parameters represent experiments of solidification of aqueous ammonium chloride solution. The marginal stability curves using the no-slip ($\overline{D}w^*=0$) and free conditions ($\overline{D}^2w^*=0$) at the liquid-mush interface are also shown. The minimum values of the Darcy-Rayleigh number R_m^* determine the critical conditions for the onset of convection in liquid and mushy layers. The curves have two minimum points except the curve derived by using the free condition. These two minima correspond to two modes of instability: a boundary-layer mode with a smaller wavelength comparable to the compositional boundary-layer thickness above the mush, and a mushy-layer mode with a large wavelength comparable to the mushy-layer

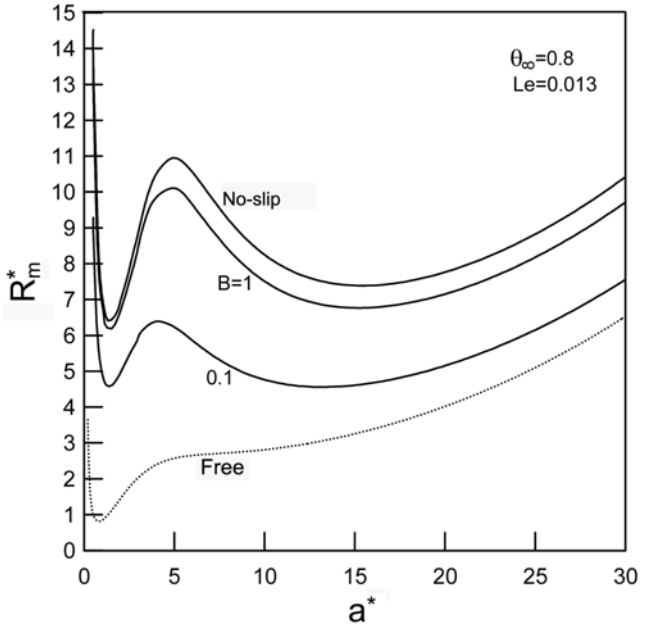

Fig. 3. Marginal stability curves using Beavers-Joseph condition for St=5, γ=20, θ_∞=0.8 and Le=0.013.

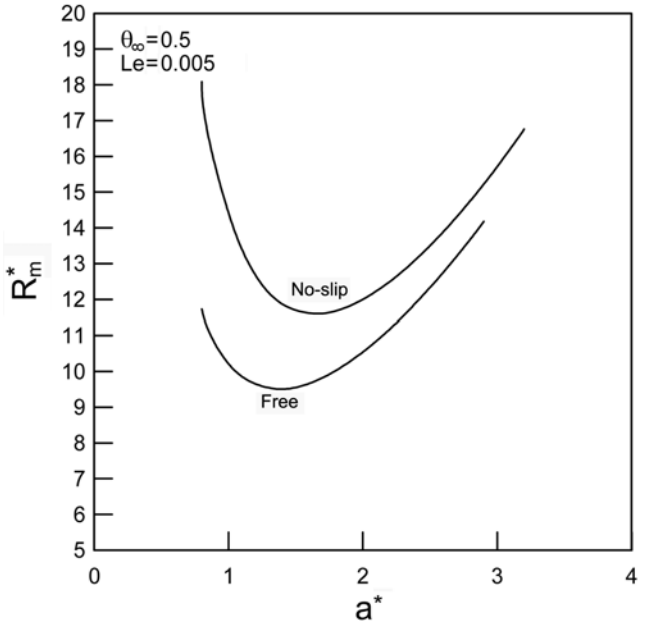

Fig. 4. Marginal stability curves using no-slip and free conditions for St=5, γ=20, θ_∞=0.5 and Le=0.005.

thickness. It is seen from Fig. 3 that the critical Darcy-Rayleigh number $R^*_{m,c}$ decreases with decreasing the value of a constant B, and therefore the inclusion of slip velocity at the liquid-mush interface destabilizes the binary melt in directional solidification. Lu and Chen [12] performed a linear stability analysis of steady solidification using the Beavers-Joseph condition with B=0.1. In Fig. 4 the marginal stability curves for the mushy-layer-mode of convection are shown for St=5, γ=20, θ_∞=0.5 and Le=0.005. The no-slip condition leads to a smaller increase of the critical Darcy-Rayleigh number than the free condition. The Beavers-Joseph condition is more appropriate for the boundary-layer mode of convection, compared with the restrictive no-slip condition.

For the mushy-layer-mode of instability in the case of Le→0, the no-slip condition ($\overline{D}w^*=0$) is applied to the liquid-mush interface. In this case, the critical Darcy-Rayleigh number and wave number are found to be $R^*_{m,c}$ and a^*_c=1.60 for St=5, γ=20, θ_∞=0.5. When the perturbation of the liquid-mush interface conditions is not considered, conditions (21) and (22b) are converted into $\overline{D}\theta^*=A\overline{D}\theta^*_m$ and $\chi^*=0$, respectively, and the critical values for St=5, γ=20, θ_∞=0.5 are $R^*_{m,c}$=10.8 and a^*_c=1.57 (from Hwang and Choi [23]). The perturbed interface conditions lead to an increase of the critical values, but their effects on the convective instability are very small. In the limit of Le→0, we found $R^*_{m,c}$- and a^*_c-values for experimental parameters of Chen and Chen [5], as shown in Fig. 5. The Lewis number has the order of 10^{-2} for aqueous ammonium chloride solution. For a small Lewis number mushy-layer-mode convection predominates, as discussed by Worster [6]. Chen and Chen [5] observed plume convection in 26% ammonium chloride-water solution when the temperature of the bottom boundary T_B is lower than 12 °C. The eutectic temperature is −15.4 °C, and for C_∞=26% the liquidus temperature $T_L(C_\infty)$ is 15 °C. When the temperature difference is defined by $\Delta T=\Gamma\Delta C=T_L(C_\infty)-T_B$, the present $R^*_{m,c}$ ranges from 7.6 to 15.1 for $0.206\le\theta_\infty\le2.4$ or $-31.5\,^\circ C\le T_B\le11\,^\circ C$; the range of St is $3.18\le St\le24.2$ and the range of γ is $11.6\le\gamma\le87.9$. The superheat (or the initial temperature of the melt) θ_∞ increases as the temperature of the bottom boundary T_B increases. As shown in Fig. 5, the critical Darcy-Rayleigh number decreases with increasing θ_∞, and therefore θ_∞ has a stabilizing effect. When T_B (or θ_∞) is high, the phase change rate λ of the mushy layer is small. Fig. 6 shows that $R^*_{m,c}$ decreases with decreasing λ or increasing T_B. Chen and Chen [5] estimated the critical solute Rayleigh number across the mush R_{mS} ($=g\beta_m\Delta C\Gamma H/D\nu$) for the onset of plume convection to be between 200 and 250. The relation between R^*_m and R_{mS} is $R^*_m/R_{mS}\approx O(10^{-2})$ since $D/\kappa\approx O(10^{-2})$.

Based on Amberg and Homsy's [8] model, in which a mushy layer is confined between two isothermal boundaries, we examine the convective instabilities within the mushy layer. The liquid-mush interface is the upper boundary and the cooled boundary is the lower one. We consider the case of St=0, simplifying the numerical calculations and focusing on the effect of λ. Then Eqs. (11)-(13) for the mushy layer reduce to

$$(\overline{D}^2+2\lambda^2\zeta\overline{D}-a^{*2})\theta^*_m=R^*_m w^*_m\overline{D}\theta_{m0}, \tag{27}$$

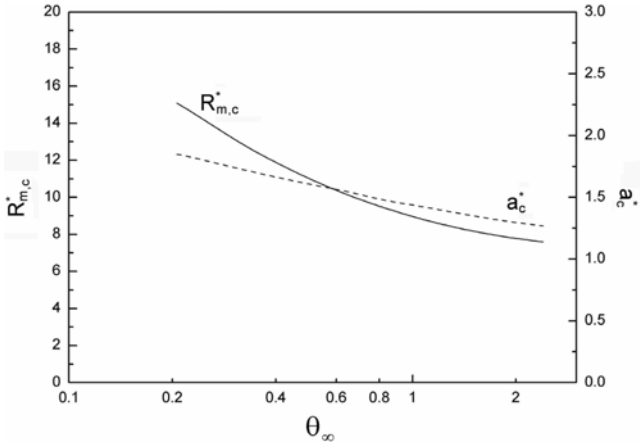

Fig. 5. Critical Darcy-Rayleigh number $R^*_{m,c}$ and critical wave number a^*_c as a function of θ_∞ for 26% NH_4Cl-H_2O solution.

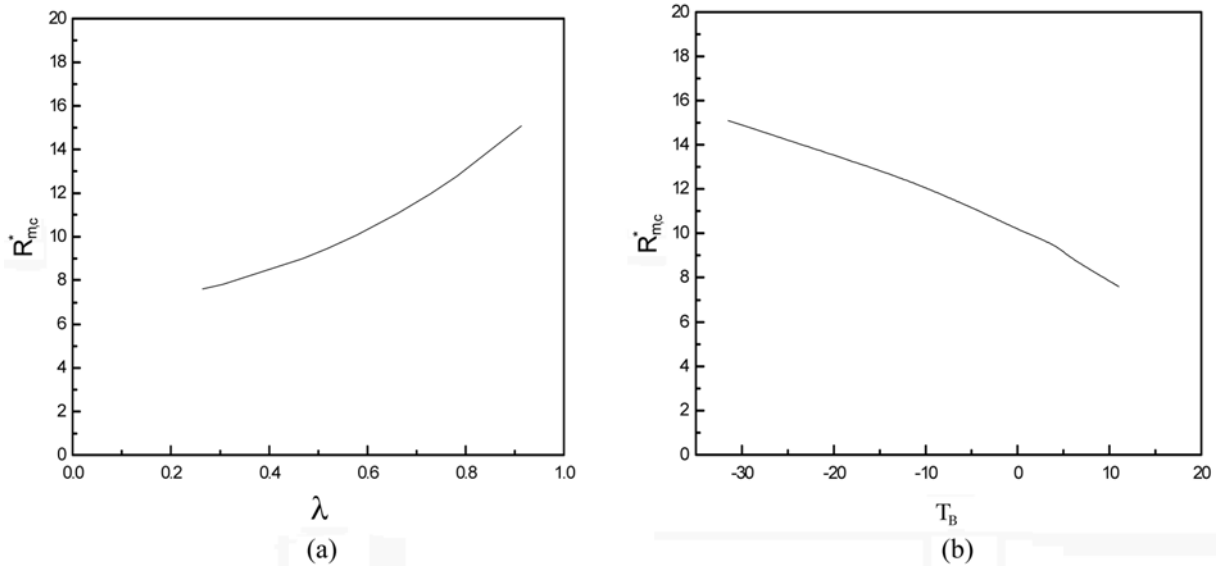

Fig. 6. Effects of (a) λ and (b) T_B on critical Darcy-Rayleigh number $R^*_{m,c}$ for 26% NH_4Cl-H_2O solution.

$$(\overline{D}^2 - a^{*2})w_m^* = a^{*2}\theta_m^*. \quad (28)$$

The boundary conditions at the liquid-mush interface are modified to be $\theta_m^*=0$, $\overline{D}w_m^*=0$ and $\chi^*=0$ at $\zeta=1$. The equation $\overline{D}w_m^*=0$ is the constant-pressure boundary condition, which was used by Chung and Chen [14], and Govendor [28]. The boundary conditions at the mush-solid interface are the same as Eqs. (26a) and (26b). Amberg and Homsy [8], and Anderson and Worster [11] used $w_m^*=0$ instead of $\overline{D}w_m^*=0$ at $\zeta=1$, assuming the liquid-mush interface to be rigid and impermeable. A detailed discussion of a permeable liquid-mush interface is found in Roper et al. [13]. The phase-change rate, λ, plays an important role in the convective instabilities of the mushy layer in time-dependent solidification. For a large λ (>3) the critical values are found to be directly proportional to λ: $R_{m,c}^*=25.9\lambda$ and $a_c^*=1.80\lambda$. For $\lambda=0.01$, the critical values are found to be $R_{m,c}^*=27.098$ and $a_c^*=2.326$. For $\lambda\rightarrow 0$, the present predictions approach the results of the stability analysis of the horizontal porous layer with a linear temperature gradient [27].

CONCLUSION

We have investigated theoretically the onset of compositional convection in directional solidification systems, where the mushy layer is growing from below. We have found the critical conditions using the self-similar stability equations for the liquid and mushy layers, based on the propagation theory. The no-slip condition applied to the liquid-mush interface suppresses the onset of convection, compared with the Beavers-Joseph condition which is appropriate for the boundary-mode of convection. When the Lewis number goes zero, the critical conditions for the mushy-layer-mode of convection are found for experiments of 26% ammonium chloride-water solution. The critical Darcy-Rayleigh number decreases with increasing the temperature of the bottom boundary or with decreasing the phase-change rate of the mushy layer. The propagation theory we have developed produces reasonable stability criteria for the onset of natural convection in directional solidification of a binary melt.

REFERENCES

1. A. C. Fowler, *IMA J. Appl. Math.*, **35**, 159 (1985).
2. F. Chen and C. F. Chen, *J. Fluid Mech.*, **207**, 311 (1989).
3. H. E. Huppert, *J. Fluid Mech.*, **212**, 209 (1990).
4. S. H. Davis, *J. Fluid Mech.*, **212**, 241 (1990).
5. C. F. Chen and F. Chen, *J. Fluid Mech*., **227**, 567 (1991).
6. M. G. Worster, *J. Fluid Mech*., **237**, 649 (1992).
7. S. Tait and C. Jaupart, *J. Geophys. Res*., **97**, 6735 (1992).
8. G. Amberg and G. M. Homsy, *J. Fluid Mech*., **252**, 79 (1993).
9. P. W. Emms and A. C. Fowler, *J. Fluid Mech*., **262**, 111 (1994).
10. F. Chen, J. W. Lu and T. L. Yang, *J. Fluid Mech*., **276**, 163 (1994).
11. D. M. Anderson and M. G. Worster, *J. Fluid Mech.*, **302**, 307 (1995).
12. J. W. Lu and F. Chen, *J. Cryst. Growth*, **171**, 601 (1997).
13. S. M. Roper, S. H. David and P. W. Voorhees, *J. Fluid Mech*., **596**, 333 (2008).
14. C. A. Chung and C. F. Chen, *J. Fluid Mech.*, **408**, 53 (2000).
15. I. G. Hwang and C. K. Choi, *J. Cryst. Growth*, **162**, 182 (1996).
16. I. G. Hwang and C. K. Choi, *J. Cryst. Growth*, **220**, 326 (2000).
17. I. G. Hwang and C. K. Choi, *J. Cryst. Growth*, **267**, 714 (2004).
18. M. C. Kim, D. Y. Yoon and C. K. Choi, *Korean J. Chem. Eng.*, **13**, 165 (1996).
19. C. K. Choi, K. H. Kang, M. C. Kim and I. G. Hwang, *Korean J. Chem. Eng.*, **15**, 192 (1998).
20. D. Y. Yoon, M. C. Kim and C. K. Choi, *Korean J. Chem. Eng.*, **20**, 27 (2003).
21. M. C. Kim, T. J. Chung and C. K. Choi, *Korean J. Chem. Eng.*, **21**, 69 (2004).
22. T. J. Chung, M. C. Kim and C. K. Choi, *Korean J. Chem. Eng.*, **21**, 41 (2004).
23. I. G. Hwang and C. K. Choi, *Korean J. Chem. Eng.*, **25**, 199 (2008).
24. C. K. Choi, J. H. Park, M. C. Kim, J. D. Lee, J. J. Kim and E. J. Davis, *Int. J. Heat Mass Transfer*, **47**, 4377 (2004).
25. C. K. Choi, J. H. Park, H. K. Park, H. J. Cho, T. J. Chung and M. C. Kim, *Int. J. Thermal Sci.*, **43**, 817 (2004).
26. G. S. Beavers and D. D. Joseph, *J. Fluid Mech*., **30**, 197 (1967).
27. D. A. Nield and A. Bejan, *Convection in porous media*, Springer-Verlag, New York (1977).
28. S. Govender, *Transp. Porous Med*., **67**, 431 (2007).